Journal of Ecohumanism
2024
Volume: 3, No: 7, pp. 2417 – 2433
ISSN: 2752-6798 (Print) | ISSN 2752-6801 (Online)
https://ecohumanism.co.uk/joe/ecohumanism
DOI: https://doi.org/10.62754/joe.v3i7.4647

# Spatiotemporal Prediction of Future LULC Changes, Northern and Northeastern Parts of Iraq with MOLUSCE

Noor Q.Sabri[1], Thair S. Khayyun[2]

**Abstract**

*The objective of this study was to develop a model for predicting future alterations in land use as well as land cover (LULC) within the low folded zone of Iraq by utilizing remote sensing data spanning for the period from 2000 to 2020. An integrated Cellular Automata-Artificial Neural Network (CA-ANN) methodology which is provided by the Molusce Plugin model in QGis was employed to produce Land Use and Land Cover (LULC) maps for the years 2020, 2040, 2060, and 2100. The results of the validation K (overal)= 0.83499, K(location)= 0.8586, K(histo) = 0.97245, % of correctness =93.044 and $R^2$= 0.9997 demonstrated a high level of concordance between the classed maps and the maps generated by the model. Future predictions demonstrate that the built-up land will increase (from 2481.95 to 16347.77 km²), barren land, water bodies, (Dense, Sparse) vegetation, Plantation, and Agricultural fallow and Agricultural land will decrease (from 22595.4 to 19129.18 km²), (from 672.1 to 562.29 km²), (from 1059.83 to 425.73 km²), (from 962.50 to 320.20 km²), (from 1196.75 to 428.5 km²), (from 15172.0389 to 10644.1551 km²) and (from15877.071 to 12408.32 km²) respectively. The decrease in the future agricultural land will impact the water and food security of this zone.These forecasts can assist in recognizing probable ecological consequences, such as alterations in water availability, agricultural stability, and the depletion of natural habitats. In general, MOLUSCE is a beneficial instrument for forecasting and evaluating forthcoming changes in land use and land cover (LULC), as well as aiding in the promotion of sustainable land use planning endeavors. The implications of the findings are significant for a range of stakeholders, such as urban planners, policymakers, environmental scientists, conservation biologists, non-governmental organizations (NGOs), and water resources managers.*

**Keywords:** *Land Use, Land Cover, MOLUSCE, Qgis, (CA-ANN), Remote Sensing.*

## Introduction

Alterations in land use and land cover (LULC) exert a substantial and immediate impact on both local and global environments, leading to climate change, deterioration of ecosystem services, and land degradation [1]. Due to the swift increase in the global population and the advancement of society, the speed and magnitude of these transformations have surpassed historical rates, resulting in significant disturbances to Earth's landscapes [2]. On a global scale, urban land area has expanded by 346.4 thousand km² at a growth rate of 1.3% between 1992 and 2016 [3]. Furthermore, given the current patterns in population density change, it is anticipated that by 2030, urban land cover will increase by 1.2 million km². [4]. As a result, precise measurement and forecasting of LULC changes in the present and the future are essential for efficient environmental management and long-term planning.

Satellite remote sensing data has gained prominence with the advancement of satellite sensors, providing frequent and comprehensive spatial and temporal coverage for monitoring LULC changes. Geospatial modelling techniques have been employed in several studies to estimate future changes in land use and land cover (LULC) by considering present circumstances and influential factors like population growth and environmental stressors [5-8]. To unravel the mechanisms driving LULC changes, various modeling techniques have rapidly progressed in terms of spatial analysis, simulation, and predicting transition potentials. Simulation models that are effective and reproducible play a crucial role in understanding the determinants and projections of past, present, and future LULC changes across different contexts. Researchers have proposed several spatially distributed models, such as Dinamica [9], Markov-FLUS [10], SLEUTH cellular automata [11], artificial neural network-Markov chain [12], CA-ANN [13], and CLUE-S [14], to analyze and project LULC changes. Each model offers a unique approach to address the complexities of LULC changes. Neural network models, known for their ability to accurately capture

[1] Civil Engineering Department, University of Technology, Baghdad-Iraq [1], Email: bce.19.86@grad.uotechnology.edu.iq, (Corresponding Author)
[2] Civil Engineering Department, University of Technology, Baghdad-Iraq, Email: 40073@uotechnology.edu.iq.

Journal of Ecohumanism
2024
Volume: 3, No: 7, pp. 2417 – 2433
ISSN: 2752-6798 (Print) | ISSN 2752-6801 (Online)
https://ecohumanism.co.uk/joe/ecohumanism
DOI: https://doi.org/10.62754/joe.v3i7.4647

nonlinear spatially probabilistic land-use transformations, are popular for simulating LULC changes [15]. Cellular automata (CA) models are effective tools for understanding land-use systems and the dynamics that underlie them, especially in conjunction with other methods like ANN. The CA-ANN model, leveraging "what-if" scenarios, finds applications in development and land change simulation studies [16–18] Artificial Neural Networks (ANN) may effectively address challenges emerging from diverse sources by employing nonparametric, nonlinear, and stochastic approaches for modelling and predicting Land Use and Land Cover (LULC) changes. The ANN's capacity to learn from diverse datasets enabled the model to effectively navigate intricate settings in the simulation. [19]. Along with geospatial technology and big data from remote sensing, traditional approaches based on change detection mechanisms and historical records are used to identify trends in the landscape and produce reliable scientific results and policy recommendations. In especially in quickly growing metropolitan areas, these strategies help planners and authorities promote sustainable development [20-22]. Consequently, transitional potential modeling and anticipating future LULC changes under the influence of geographical variables aim to identify past and potential future change locations. Most of these models employ temporal land-use data and incorporate geographical characteristics to forecast future LULC scenarios [23].

Both anthropogenic and natural events, such as war and drought, have had a considerable impact on LULC in Iraq during the past few decades, leading to significant changes in the region [24, 25]. However, an accurate estimation of LULC in the low folded zone- Iraq is currently lacking, and official Iraqi government statistics may be unreliable [26]. In this study, the Modules for Land-Use Change Simulation (MOLUSCE) plugin within QGIS (an open-source model) was employed to analyze, model, and simulate LULC changes. The plugin incorporates various algorithms, including artificial neural networks (ANNs), multi-criteria evaluation (MCE), weights of evidence (WoE), logistic regression (LR), and Monte Carlo cellular automata (CA) models. By utilizing the CA-ANN technique and remotely sensed big data from 2000 to 2020 with a ten-year interval, simulated spatiotemporal transitioning possibilities and predicted future LULC changes for the years 2040, 2060, 2080, and 2100. The spatiotemporal change analysis and prediction of future changes in land use and land cover are evaluated for the first time in this research in the Low Folded Zone, Iraq. The findings of this study offer valuable insights for land use planners to enhance their decision-making process within the context of sustainable land use planning.

## Materials and Methods

*Study Area*

The Low Folded Zone comprises a significant portion, specifically 13.6%, of Iraq's total geographical area, covering a vast expanse measuring 56930 square kilometers. The geographical position of the region is situated in the north and northwest central regions of Iraq, as illustrated in Figure 1a. The topography of this region exhibits a gradual elevation gradient, commencing from the southwestern boundary at an elevation range of 125 to 300 meters above mean sea level, and progressively ascending toward the northern and eastern perimeters, where it attains altitudes that range from 900 to one thousand meters above mean sea level. The geographical area being examined includes many notable aquifers, specifically the Fatha, Injana, Mukdadiyah, Bai Hassan Constructions, and Quaternary deposits [27]. The Low Folded Zone consists of thirteen sub-provinces, as seen in Figure 1b.

Journal of Ecohumanism
2024
Volume: 3, No: 7, pp. 2417 – 2433
ISSN: 2752-6798 (Print) | ISSN 2752-6801 (Online)
https://ecohumanism.co.uk/joe/ecohumanism
DOI: https://doi.org/10.62754/joe.v3i7.4647

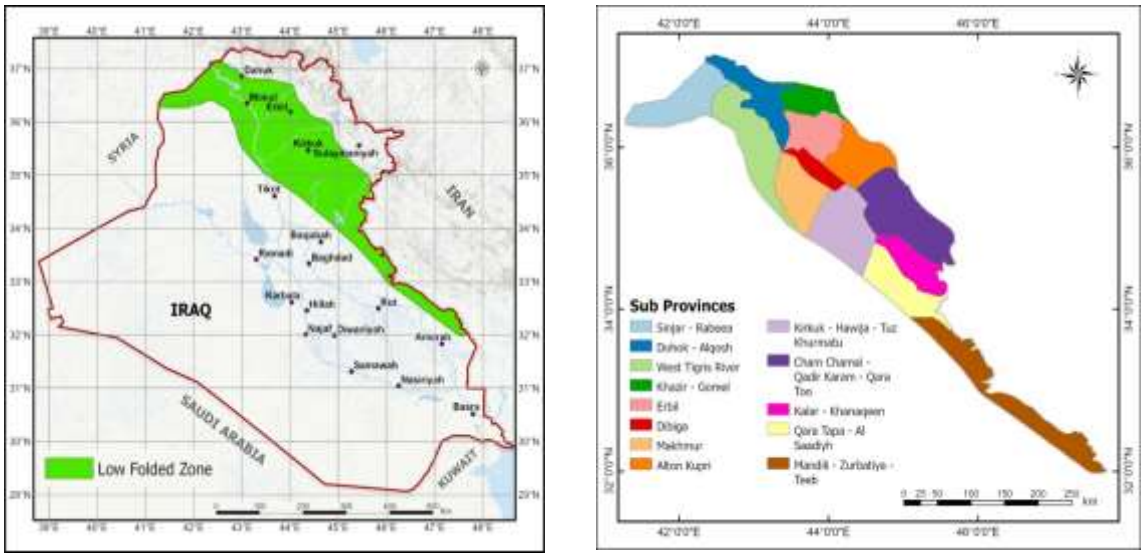


**Figure 1:** (A) Location Map of The Study Area And (B) Sub-Provinces of The Study Area.

*Dataset*

Landsat satellite images from three years prior, specifically from 2000, 2010 and 2020, makes up the dataset used in this study. The imagery displaying the least amount of cloud cover were acquired from the Earth Explorer site, which was maintained by the US Geological Survey (USGS).

*Dataset Pre-Processing and Classification*

Before performing the classification procedure, the satellite images were subjected to rectification for radiative and environmental noises using the FLASH settings (atmospheric correction tool in remote sensing) of the environment 5.2 platforms. The rectification process plays a critical role in obtaining accurate numeric surface data from the image. The coefficients obtained from the picture data were employed in the rectification process [28].

The acquired imaging pictures captured within the identical temporal window and calendar year were merged utilizing a mosaic approach. Following this, the relevant study area was demarcated and separated. Different combinations of bands were employed in order to improve the accurate identification of surface features before collecting data for retraining or generating spectra signature data for categorization. The Thematic Mapper (TM) employed the band arrangement of RGB 4, 3, 2, whereas the Operational Land Imager (OLI) utilized the band mixture of RGB 5, 4, 3. The classification of various land use and cover (LULC) classes was conducted by the researchers, who considered the professional knowledge of the research area's physiography, together with relevant additional data. The data presented aided in the process of delineating and discerning the probable feature categories through the utilization of the training samples. The study classified many types of land use and cover (LULC) groups, including heavy vegetation, sparse vegetation, agricultural land, abandoned agricultural land, plantation, built-up areas, and barren terrain. The aforementioned classes are displayed in Table 1.

This table provides descriptions of different classes of land cover and land use (LCLU) observed within the research region.

Journal of Ecohumanism
2024
Volume: 3, No: 7, pp. 2417 – 2433
ISSN: 2752-6798 (Print) | ISSN 2752-6801 (Online)
https://ecohumanism.co.uk/joe/ecohumanism
DOI: https://doi.org/10.62754/joe.v3i7.4647

**Table 1:** Description of the LCLU Classes

| Class | Description |
|---|---|
| **Built-up area** | Settlements: Man-made Infrastructure |
| **Barren land** | Barren landscapes devoid of conspicuous vegetation, particularly lacking any discernible clusters of trees or shrubs. The landscape consists of exposed rocks, hills, soil, barren ground, rocky formations, and open terrain devoid of vegetation. |
| **Waterbody** | Water bodies refer to several types of aquatic environments, such as rivers, fishponds, lakes, and streams. |
| **Dense vegetation** | Highly concentrated areas of vegetation, primarily consisting of forests and thick shrublands. |
| **Sparse vegetation** | Dispersed areas with sparse mixed forests, shrublands, and patches of grassland |
| **Plantation** | The landscape consists of densely vegetated areas arranged in a structured manner, as well as woods and green spaces |
| **Agricultural land** | Presently, there is cultivated area that exhibits a noticeable verdant hue. |
| **Agricultural fallow** | The footage clearly displays croplands, although there are currently no crops present. The unique geometric features of agriculture are clearly evident. |

*Methods and Inputs*

In this study, the MLP-ANN learning technique of the Cellular Automata (also known as the CA model) was employed to incorporate Land Use and Land Cover (LULC) alterations, which were characterized by transition probabilities. The method of predicting land use and land cover (LULC) in eight stages was conducted using Quantum GIS, a geographic information system software, together with the MOLUSCE plugins [29]. The initial step involved incorporating land use and land cover (LULC) shift maps for the initial year (2010) and final year (2020) into the model. A LULC change map was generated to depict the patterns of transformation in the research area between 2010 and 2020, utilizing data compiled from various sources including the Digital Elevation Model (the DEM), aspect ratio map, slope chart, and Euclidean distance.

The United States Geological Survey (USGS) provided a raster image format with a single pixel quality of 30 meters, from which the classified land use and land cover (LULC) maps were obtained. The subsequent stages of the model were dependent on the utilization of these maps as their primary source of input. The MLP-ANN plugins (multilayer perception) were employed to forecast land use and land cover (LULC) alterations by considering the fluctuating percentage of the area over the course of multiple years. The study identified and categorized eight distinct land use types, including built-up areas, barren land, water bodies, dense vegetation, sparse vegetation, plantations land for agriculture, and agricultural wasteland. The map additionally depicted discrepancies within each of these regions.

To quantify the variation in pixel values representing different land use protections, a matrix was developed. In order to project future land use and land cover (LULC) maps, a fundamental presumption of continuity in current patterns and dynamics of LULC was used. Figure 2 illustrates the projected land use and land cover (LULC) transition map for the years 2040, 2060, 2080, to 2100. This projection is based on the analysis of classified raster images obtained from the United States Geological Survey (USGS) between 2000 and 2020.

Journal of Ecohumanism
2024
Volume: 3, No: 7, pp. 2417 – 2433
ISSN: 2752-6798 (Print) | ISSN 2752-6801 (Online)
https://ecohumanism.co.uk/joe/ecohumanism
DOI: https://doi.org/10.62754/joe.v3i7.4647

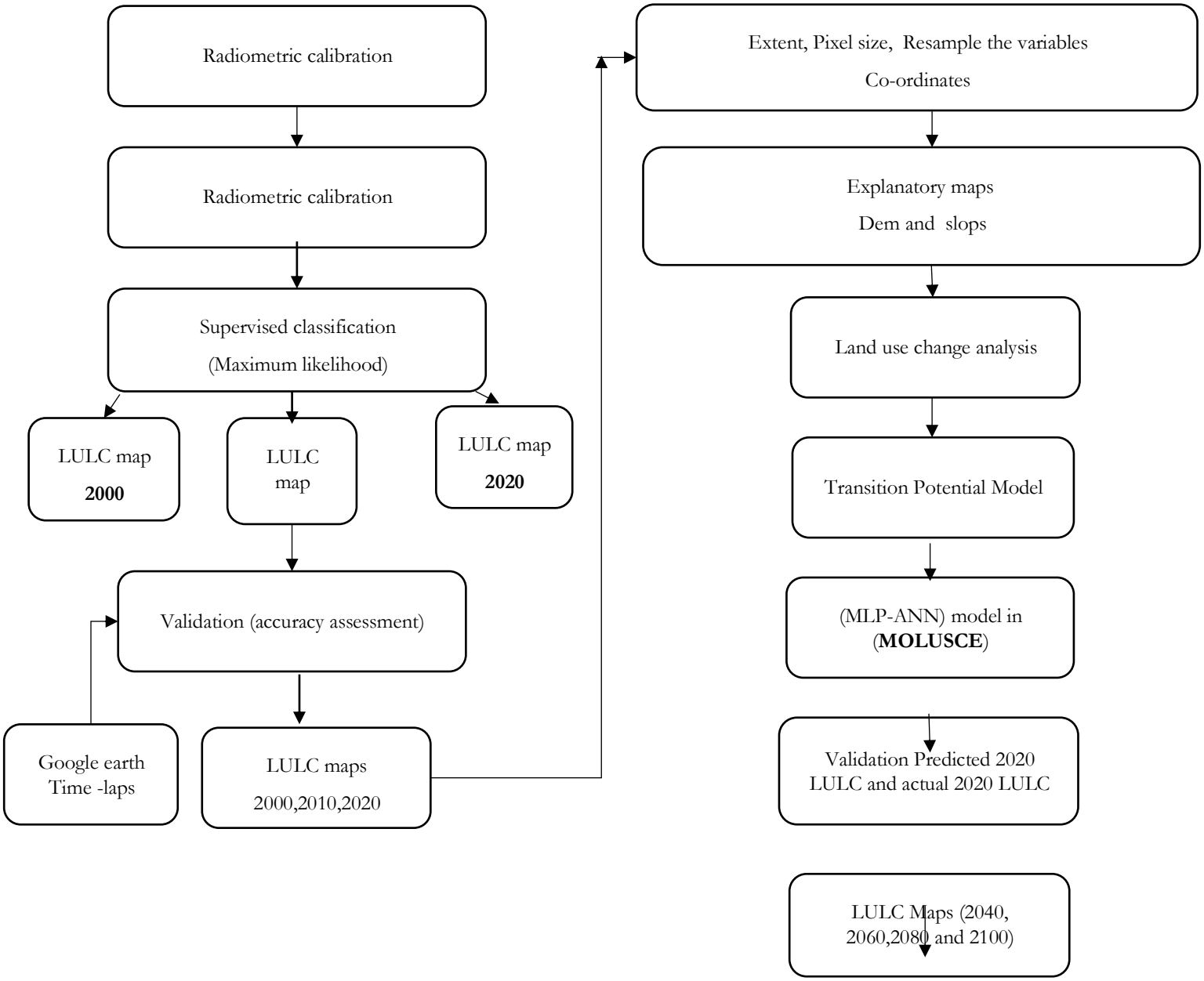


**Fig.2** Methodology Flowchart of This Research

*Evaluation Correlations and Area Change*

*MLP − ANN And Transition Potential Modeling*

The study evaluated the associations between the two raster images using statistical metrics including Pearson connection, Cramér coefficient, and joint uncertainties in data [29]. Subsequently, the changes in land use and land cover (LULC) classes were calculated for the period between 2000 and 2020. The method generated a change matrix to visually depict the variations in pixel modifications among several categories. This phase aimed to precisely quantify the changes in land area, measured in square kilometers ($km^2$), that existed between the land use and land cover (LULC) classes of 2000 and 2020 [30, 31].

Journal of Ecohumanism
2024
Volume: 3, No: 7, pp. 2417 – 2433
ISSN: 2752-6798 (Print) | ISSN 2752-6801 (Online)
https://ecohumanism.co.uk/joe/ecohumanism
DOI: https://doi.org/10.62754/joe.v3i7.4647

To construct probabilistic shift maps for land use and land cover (LULC) changes, one can utilize many techniques such as MLP-ANN, WoE, LR, and Multi-Criteria Evaluation (the MCE). These methods have been employed to statistically and geographically calibrate and simulate land use and land cover changes [32, 33]. In this study the MLP-ANN forecast method was employed which was integrated as a plugin, to predict the LULC map. In order to evaluate the precision of the projected land use and land cover (LULC) maps, the Kappa factor (equations 1-3) was utilized.

$$\text{Kappa} = \frac{p_o - p_e}{1 - p_e} \qquad (1)$$

where,. Pe indicates the percentage of expected agreements, and $P_o$, indicates the percentage of actual agreements.

$$P_o = \sum_{i=1}^{c} P_{ij} \qquad (2)$$

$$P_e = \sum_{i=1}^{c} p_i T_i T_j \qquad (3)$$

A contingency table is used to visually represent the relationship between the $i^{th}$ and $j^{th}$ cells by displaying the frequency patterns of variables in a matrix format. The variables $T_i$ and $T_j$ represent the total sum of all cells in the $i^{th}$ and $j^{th}$ columns, correspondingly. At the same time, the variable c represents the number of raster categories. The contingent table is employed to calculate and arrange the relationships between individual cells, while also producing a measure for each respective cell [34].

This study combined the LULC data and MLP-ANN as resources to calibrate and model changes in land use/land cover. The enormous data uncertainty presented a substantial problem during the execution of the approach. Therefore, a continuous index spanning from 0 to 1 was used to describe the topography. The artificial neural networks utilize fuzzy logic to determine a range of values between 0 and 1, based on the usefulness of the terrain. Artificial neural networks (ANNs) rely on the interaction of interconnected neurons and the modification of synaptic interconnections among them [ 35].

*Annual Rate of Change Analysis*

To ascertain the annual pace of shift for each land use type, the magnitude of shift between successive years was computed by subtracting the initial year values from the end-year value. The quotient of this discrepancy was obtained by dividing it by the initial year value and the duration of time. Equation (4) was utilized to assess the spatial and temporal magnitude and rate of variation in land use and land cover (LULC) groups.

$$ARC\% = \frac{f_y - I_y}{I_y * t} \quad *100 \qquad (4)$$

where t is the time interval, $I_y$ , and $f_y$, are the beginning and final year areas, respectively, and ARC is the annual rate of change in LULC categories (%).

*Validation*

The validating module of MOLUSE (prediction model), was utilized to verify and confirm the produced image of 2020. The validation technique entailed a juxtaposition of the simulated image with the classified 2020 Land Use and Land Coverage (LULC) map. The core technique utilized by MOLUSE is based on a back-propagation mechanism, which is an iterative neural network approach that relies on learning. The neural network structure consists of three separate layers: the input layer, the hidden layer, and the output

Journal of Ecohumanism
2024
Volume: 3, No: 7, pp. 2417 – 2433
ISSN: 2752-6798 (Print) | ISSN 2752-6801 (Online)
https://ecohumanism.co.uk/joe/ecohumanism
DOI: https://doi.org/10.62754/joe.v3i7.4647

layer. During each iteration, every neuron within the output layer generates a transition probability, which indicates the possibility of changing between different land use classes.

By examining the transition probability values, it is possible to forecast the changes in land use and land cover (LULC) beyond one classification to another. The highest transition probability indicates the most likely new category. If a LULC type has the highest probability of transitioning, the status of the corresponding cell will not change. To evaluate the accuracy of the forecasts, many measures were calculated, such as the proportion of correct predictions (accuracy), the overall kappa factor, the histogram kappa factor, and the local kappa coefficient. Once a satisfactory level of precision was achieved, the cellular automata simulation step was repeated to forecast future changes in the LULC.

## Result and Discussion

*Spatiotemporal Change Analysis*

In order to check and validate the 2020 image, the verification module of the prediction model MOLUSE was used. the categorization of 2020 LULC map next to the simulated image was used in the validation procedure. An incremental neural network forms the basis of the MOLUSE algorithm's back-propagation learning method. There are three distinct layers that make up a neural network: input, hidden, and output. Every output layer neuron calculates a transition probability throughout each cycle, which represents the likelihood of switching between land use groups.

LULC maps for this study were created by classifying Landsat satellite images. For the years 2000, 2010, and 2020, three LULC maps were made to depict the low folded zone. The maps can be seen in Figures 3a, 3b, and 3c.

The data of the LuLc area and annual rates of change are shown in details presented in Table 2 for each seven legends. As shown in Figure 3, the fast expansion of the built-up area was the primary driver of the major change in land use that occurred throughout the research period. The Built-up area grew substantially, increasing from 986.39 km² to 2481.95 km² during (2000-2020), at a pace of 7.58% each year. The extent of barren land rose from 22,293.12 km² to 22,595.41 km², which represents an increase of 0.067% each year. Plantation, agricultural land, and Agricultural fallow increased significantly during the years 2000,2010 and 2020. All these parameter values were within a range of (934.81 to 1196.74 km²), (14,954.39 to 15,172.03 km²), and (15,483.12 to 15,877.1 km²), respectively.

As a counterpoint, the Waterbody region had a decline of 672.11 km², which represents a loss rate of 0.64% per year (from 770.77 to 672.11 km²). The amount of dense vegetation decreased from 3994.1 km² to 1059.83 km² during the period 2000 to 2020, while the area of sparse vegetation reduced from 1156.53 km² to 962.50 km².

Journal of Ecohumanism
2024
Volume: 3, No: 7, pp. 2417 – 2433
ISSN: 2752-6798 (Print) | ISSN 2752-6801 (Online)
https://ecohumanism.co.uk/joe/ecohumanism
DOI: https://doi.org/10.62754/joe.v3i7.4647

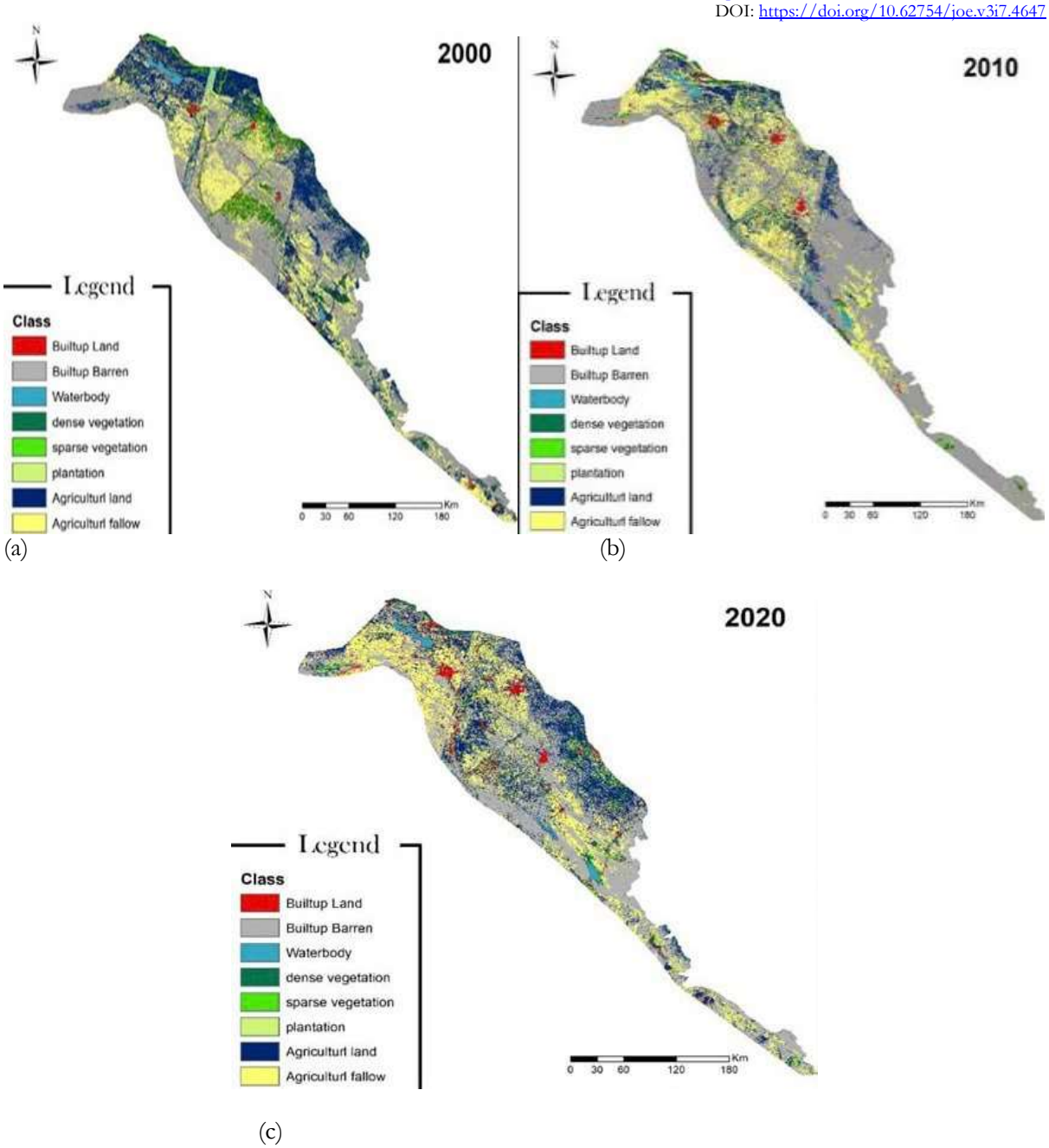


**Fig. 3** LULC maps for a) 2000, b) 2010 and c) 2020

**Table 2.** LULC Area And Annual Rate of Change (ARC) For the Periods 2000-2020.

| LULC Type | 2000 | | 2010 | | 2020 | | ARC % |
|---|---|---|---|---|---|---|---|
| | km² | % | km² | % | km² | % | |
| **Built-up area** | 986.39 | 1.63 | 1434.79 | 2.39 | 2481.95 | 4.14 | 7.580956413 |
| **Barren land** | 22293.12 | 36.80 | 29596.20 | 49.31 | 22595.42 | 37.65 | 0.067799585 |
| **Waterbody** | 770.78 | 1.27 | 673.17 | 1.12 | 672.11 | 1.12 | -0.640020411 |
| **Dense vegetation** | 3994.09 | 6.59 | 1105.49 | 1.84 | 1059.84 | 1.77 | -3.673244883 |
| **Sparse vegetation** | 1156.54 | 1.91 | 823.41 | 1.37 | 962.50 | 1.60 | -0.838859089 |
| **Plantation** | 934.82 | 1.54 | 531.57 | 0.89 | 1196.75 | 1.99 | 1.400975462 |
| **Agricultural land** | 14954.40 | 24.69 | 9312.60 | 15.52 | 15172.04 | 25.28 | 0.072768734 |
| **Agricultural fallow** | 15483.13 | 25.56 | 16538.83 | 27.56 | 15877.07 | 26.45 | 0.127217626 |

Journal of Ecohumanism
2024
Volume: 3, No: 7, pp. 2417 – 2433
ISSN: 2752-6798 (Print) | ISSN 2752-6801 (Online)
https://ecohumanism.co.uk/joe/ecohumanism
DOI: https://doi.org/10.62754/joe.v3i7.4647

*Change in the Probability Matrix*

The values of the probability matrix's elements for the LULC categories were altered for the years 2000–2020. With the exception of the high values for the diagonal cells, which stay in their original category, Table 3 demonstrates that higher values signal more significant changes.

**Table (3)**. Probability Matrix Values for the Lulc Elements From 2000 to 2020

| Class | Built-up area | Barren land | Waterbody | Dense vegetation | Sparse vegetation | Plantation | Agricultural land | Agricultural fallow | Sum |
|---|---|---|---|---|---|---|---|---|---|
| Built-up area | 0.522 | 0.149 | 0.004 | 0.021 | 0.012 | 0.012 | 0.186 | 0.095 | 1 |
| Barren land | 0.022 | 0.517 | 0.000 | 0.008 | 0.010 | 0.013 | 0.227 | 0.202 | 1 |
| Waterbody | 0.026 | 0.007 | 0.828 | 0.073 | 0.026 | 0.014 | 0.022 | 0.006 | 1 |
| Dense vegetation | 0.074 | 0.110 | 0.037 | 0.254 | 0.097 | 0.090 | 0.246 | 0.094 | 1 |
| Sparse vegetation | 0.072 | 0.161 | 0.021 | 0.093 | 0.120 | 0.085 | 0.263 | 0.184 | 1 |
| Plantation | 0.067 | 0.124 | 0.016 | 0.085 | 0.063 | 0.137 | 0.254 | 0.253 | 1 |
| Agricultural land | 0.046 | 0.187 | 0.002 | 0.021 | 0.022 | 0.029 | 0.374 | 0.318 | 1 |
| Agricultural fallow | 0.027 | 0.302 | 0.001 | 0.009 | 0.011 | 0.016 | 0.246 | 0.387 | 1 |

*Model Validation*

Some of the algorithms used to describe transition potential in the MOLUSCE plugin include cellular automaton (CA), multicriteria assessment, logistic regression (LR), weights of proof, and multilayer perceptron (ANN). In order to model and predict the possibility of transitions, the current study employed the CA-ANN approach.

For the purpose of model calibration, spatial variables were selected for inclusion in the model, if they showed a statistically significant connection with LULC, as assessed by Cramer's coefficient. To make LULC predictions for the year 2020 as shown in figure 4, LULC data was used from 2000–2010 in conjunction with the geographical considerations. Following this, the anticipated LULC was compared with the actual LULC data for the year 2020. The model's validation results were quite good, with a 93.044% accuracy kappa, an overall kappa of 0.83499, a kappa value that was location-specific of 0.85865, and a kappa value that was histogram-specific of 0.97245 as shown in Table 4 and Figure 5. These outcomes show how reliable the model validation will use for future issues.

The model was quite good for predicting the presence of various land types. Figure 5 shows the current and projected LULC map values for the period 2020 and the Kappa statistics

Journal of Ecohumanism
2024
Volume: 3, No: 7, pp. 2417 – 2433
ISSN: 2752-6798 (Print) | ISSN 2752-6801 (Online)
https://ecohumanism.co.uk/joe/ecohumanism
DOI: https://doi.org/10.62754/joe.v3i7.4647

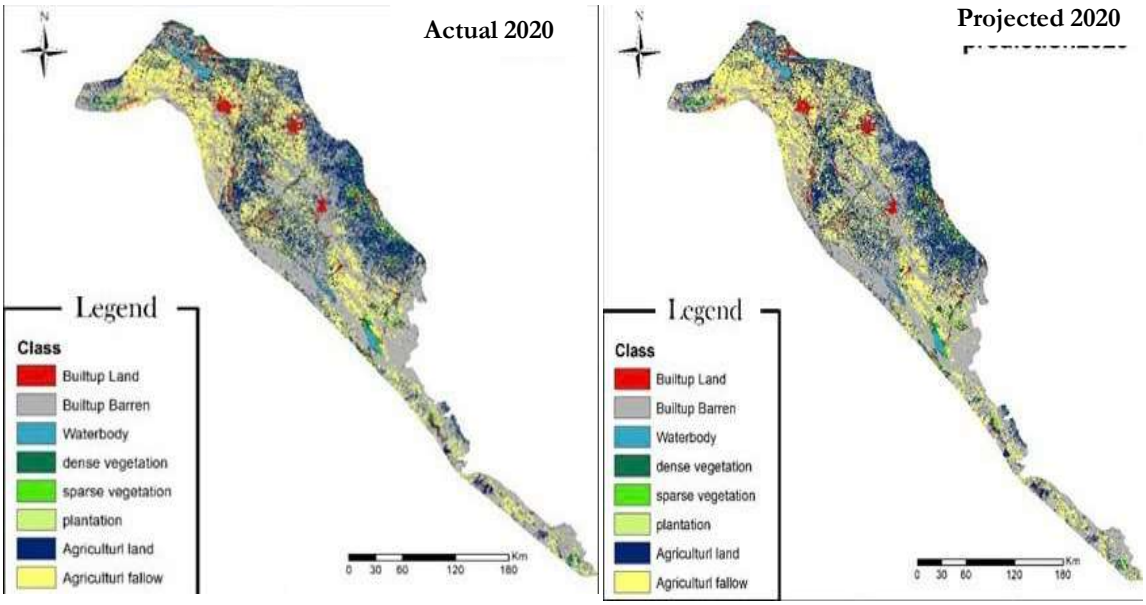


**Fig 4.** Actual and Projected LULC 2020

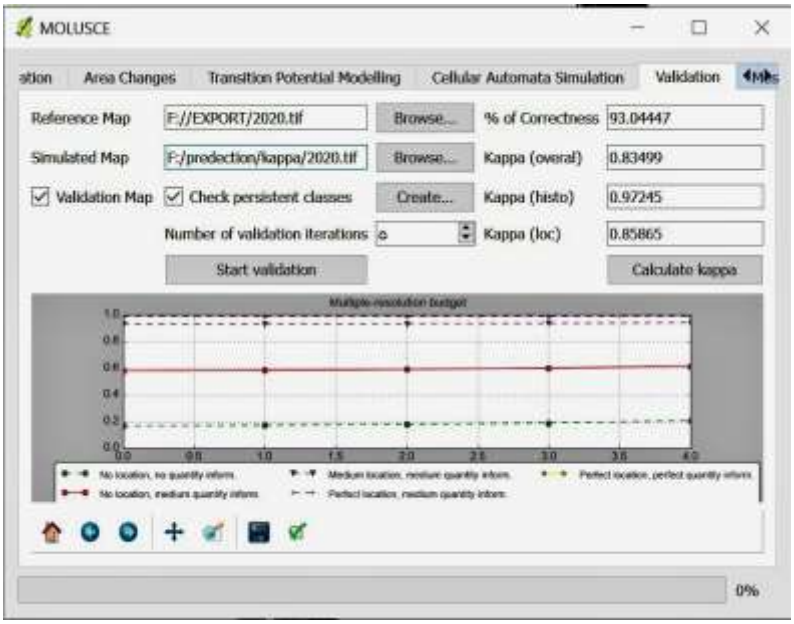


**Fig. 5** Comparison of The LULC Observed Data with The Predicted Data for The Year 2020.

Journal of Ecohumanism
2024
Volume: 3, No: 7, pp. 2417 – 2433
ISSN: 2752-6798 (Print) | ISSN 2752-6801 (Online)
https://ecohumanism.co.uk/joe/ecohumanism
DOI: https://doi.org/10.62754/joe.v3i7.4647

**Table 4.** Actual and Projected LULC Of 2020.

| LULC Type | Actual | | Projected | | Kappa value | | | % of correctness |
|---|---|---|---|---|---|---|---|---|
| | km² | % | km² | % | Overal | Histo | Loc | |
| **Built-up area** | 2481.95 | 4.14 | 2438.75 | 4.07 | | | | |
| **Barren land** | 22595.42 | 37.65 | 22960.59 | 38.29 | | | | |
| **Waterbody** | 672.11 | 1.12 | 672.05 | 1.12 | | | | |
| **Dense vegetation** | 1059.84 | 1.77 | 1059.25 | 1.77 | o.834 | 0.9724 | 0.8586 | 93.044 |
| **Sparse vegetation** | 962.50 | 1.60 | 962.10 | 1.60 | | | | |
| **Plantation** | 1196.75 | 1.99 | 1196.22 | 1.99 | | | | |
| **Agricultural land** | 15172.04 | 25.28 | 14815.17 | 24.70 | | | | |
| **Agricultural fallow** | 15877.07 | 26.45 | 15864.51 | 26.45 | | | | |

By comparing the modeled LULC map to a reference map, the MOLUSE model's built-in VALIDATE module may validate it. To validate the data, several Kappa statistical variants were computed which measure the degree of agreement or disagreement between the associated class groups. Figure 5 displays the outcomes of these Kappa statistics. $R^2$, along. Figure 6 shows a comparison of the two maps, which produced an amazing $R^2$ value of 0.9997. The results are in agreement with those of an earlier study [35], which found an $R^2$ of approximately 0.90 comparing the real and simulated LULC maps. Based on the Kappa statistics and the coefficient of determination, these validation results show that the reference map and the modeled LULC map are quite accurate and in good agreement with one another.

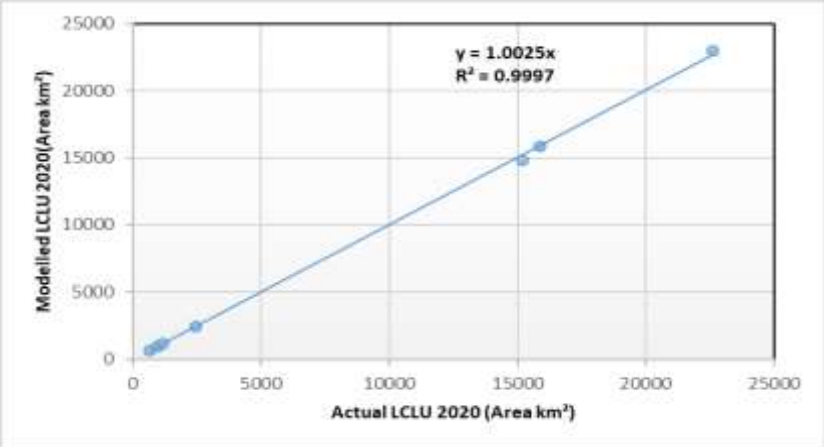


**Fig. 6** The Relationship Between the Actual and Predicted (Modeled) LULC Maps Of 2020

*Prediction of LULC*

After obtaining satisfactory results from the model validation, the future LULC for 2040, 2060,2080, and 2100 was predicted by using. the temporal LULC data from 2000 to 2020 as Figure (7), (8) and Table (5)

Journal of Ecohumanism
2024
Volume: 3, No: 7, pp. 2417 – 2433
ISSN: 2752-6798 (Print) | ISSN 2752-6801 (Online)
https://ecohumanism.co.uk/joe/ecohumanism
DOI: https://doi.org/10.62754/joe.v3i7.4647

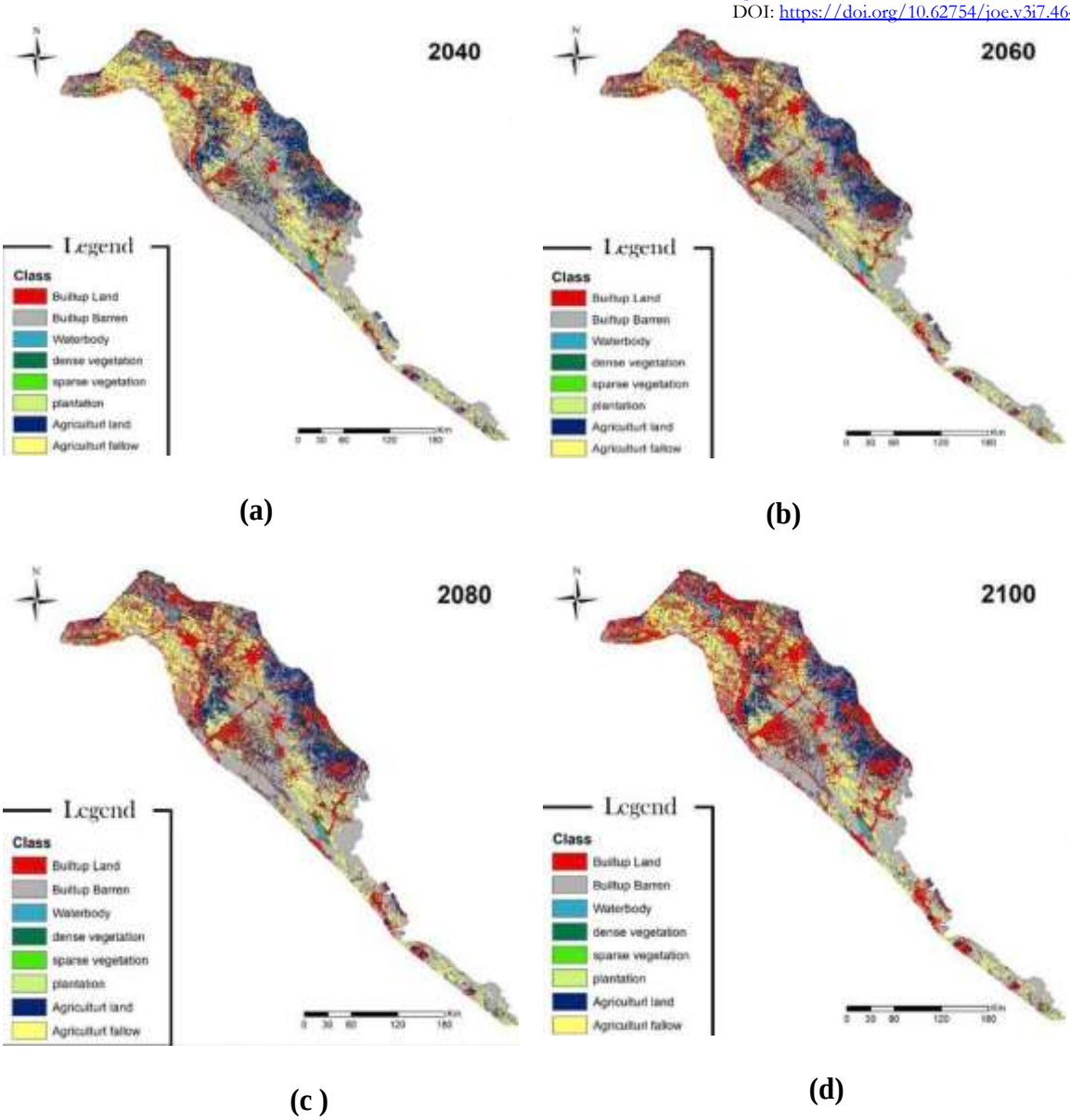


**Fig. 7** The Modeled Land Cover Land Use of Low Folded Zone (A) 2040 (B) 2060 (C) 2080 (D) 2100

Journal of Ecohumanism
2024
Volume: 3, No: 7, pp. 2417 – 2433
ISSN: 2752-6798 (Print) | ISSN 2752-6801 (Online)
https://ecohumanism.co.uk/joe/ecohumanism
DOI: https://doi.org/10.62754/joe.v3i7.4647

**Table 5.** Area and Percentage of the Prediction Land Cover Land Use Classes

| Class category | 2020 _ Area % | 2040 _ Area % | 2060 _ Area % | 2080 _ Area % | 2100 _ Area % |
|---|---|---|---|---|---|
| **Built-up area** | 4.14 | 12.69 | 18.46 | 20.79 | 27.13 |
| **Barren land** | 37.65 | 35.71 | 34.22 | 33.54 | 31.74 |
| **Waterbody** | 1.12 | 1.05 | 0.99 | 0.99 | 0.93 |
| **Dense vegetation** | 1.77 | 1.21 | 0.93 | 0.91 | 0.71 |
| **Sparse vegetation** | 1.60 | 0.99 | 0.73 | 0.71 | 0.53 |
| **Plantation** | 1.99 | 1.33 | 1.01 | 0.96 | 0.71 |
| **Agricultural land** | 25.28 | 22.35 | 20.44 | 19.69 | 17.66 |
| **Agricultural fallow** | 26.45 | 24.68 | 23.23 | 22.42 | 20.59 |

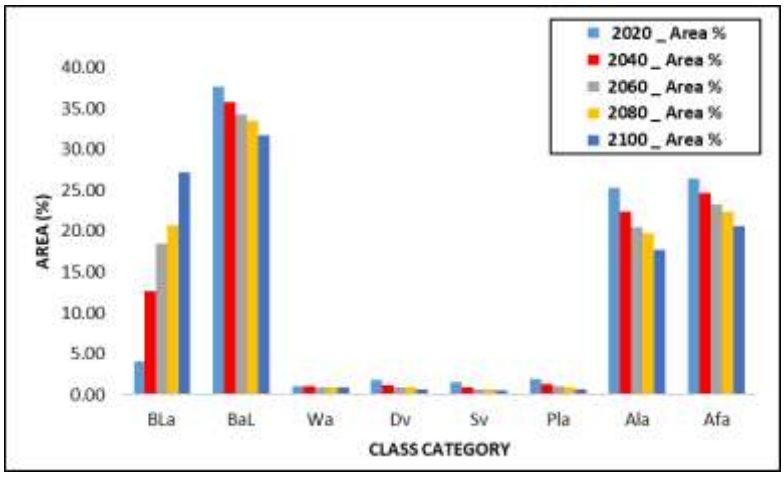


**Fig (8).** Area Percentage (%) of Changes Per Class Category for The Period 2020-2100

The changes in land cover categories from 2020 to the predicted year 2040 are summarized in Table 6. Figure 7 also provides a visual representation of these alterations. The research in this area focuses on how land area has changed relative to the total land area. An increase in area is shown by a positive change value, whereas a reduction is indicated by a negative value.

**Table 6.** Category Distributions for Lulcs Between 2020 And 2040

| class | 2020 (km²) | 2040 (km²) | change (km²) |
|---|---|---|---|
| **Built-up area** | 2481.95 | 7620.80 | 5138.85 |
| **Barren land** | 22595.42 | 21442.92 | -1152.49 |
| **Waterbody** | 672.11 | 631.65 | -40.46 |
| **Dense vegetation** | 1059.84 | 724.68 | -335.15 |
| **Sparse vegetation** | 962.50 | 595.44 | -367.06 |
| **Plantation** | 1196.75 | 797.75 | -399.00 |
| **Agricultural land** | 15172.04 | 13419.84 | -1752.20 |
| **Agricultural fallow** | 15877.07 | 14819.51 | -1057.56 |

Journal of Ecohumanism
2024
Volume: 3, No: 7, pp. 2417 – 2433
ISSN: 2752-6798 (Print) | ISSN 2752-6801 (Online)
https://ecohumanism.co.uk/joe/ecohumanism
DOI: https://doi.org/10.62754/joe.v3i7.4647

**Table 7.** Category Distributions for Lulcs Between 2020 And 2060

| class | 2020 (km²) | 2060(km²) | change (km²) |
|---|---|---|---|
| **Built-up area** | 2481.95 | 11091.76 | 8609.81 |
| **Barren land** | 22595.42 | 20564.48 | -2030.94 |
| **Waterbody** | 672.11 | 595.31 | -76.80 |
| **Dense vegetation** | 1059.84 | 560.63 | -499.21 |
| **Sparse vegetation** | 962.50 | 438.26 | -524.24 |
| **Plantation** | 1196.75 | 606.68 | -590.07 |
| **Agricultural land** | 15172.04 | 12283.05 | -2888.99 |
| **Agricultural fallow** | 15877.07 | 13959.27 | -1917.80 |

**Table 8.** Category Distributions for Lulcs Between 2020 And 2080

| class | 2020 (km²) | 2080(km²) | change (km²) |
|---|---|---|---|
| **Built-up area** | 2481.95 | 12508.17 | 10026.22 |
| **Barren land** | 22595.42 | 20173.39 | -2422.02 |
| **Waterbody** | 672.11 | 595.23 | -76.88 |
| **Dense vegetation** | 1059.84 | 545.92 | -513.92 |
| **Sparse vegetation** | 962.50 | 425.67 | -536.84 |
| **Plantation** | 1196.75 | 576.17 | -620.58 |
| **Agricultural land** | 15172.04 | 11846.77 | -3325.27 |
| **Agricultural fallow** | 15877.07 | 13483.94 | -2393.13 |

**Table 9.** Category Distributions for Lulcs Between 2020 And 2100

| class | 2020 (km²) | 2100(km²) | change (km²) |
|---|---|---|---|
| **Built-up area** | 2481.95 | 16347.77 | 13865.82 |
| **Barren land** | 22595.42 | 19129.19 | -3466.23 |
| **Waterbody** | 672.11 | 562.29 | -109.82 |
| **Dense vegetation** | 1059.84 | 425.73 | -634.11 |
| **Sparse vegetation** | 962.50 | 320.21 | -642.30 |
| **Plantation** | 1196.75 | 428.52 | -768.23 |
| **Agricultural land** | 15172.04 | 10644.16 | -4527.88 |
| **Agricultural fallow** | 15877.07 | 12408.32 | -3468.75 |

The study indicates when the future results are compared with the data of the year 2020, the built-up area has the potential to increase by 5138.85 square kilometers by 2040. On the flip side, it can be expected a decrease of 1152.49 sq. km in barren land, 40.46 sq. km in water bodies, 335.15 sq. km in dense vegetation, 367.06 sq. km in sparse vegetation, 399 sq. km in plantation, 1752.2 sq. km in agricultural fallow, and 1057.56 sq. km in agricultural land. In addition, the study sheds light on a common pattern where the growth of one type of land cover is inversely related to the shrinkage of other types, and the opposite is also true.

Moving on to the differences between 2020 and 2060, as shown in Table 7 and Figure 7, the study shows a significant increase in the extent of developed land. In particular, by 2060, the projected urbanized area will have grown from 2481.95 km² in 2020 to 11091.76 km². On the other hand, it is expected that the areas of water bodies, dense vegetation, sparse vegetation, plantation, agricultural land, and agricultural fallow will decrease widely, shifting from 22595.42 km² to 20564.48 km², 672.11 km² to 595.31 km², 1059.84 km² to 560.31 km², 962.5 km² to 438.26 km², 1196.75 km² to 606.68 km², 15172.04 km² to 12283.05 km², and 15877.07 km² to 13959.72 km², accordingly

Journal of Ecohumanism
2024
Volume: 3, No: 7, pp. 2417 – 2433
ISSN: 2752-6798 (Print) | ISSN 2752-6801 (Online)
https://ecohumanism.co.uk/joe/ecohumanism
DOI: https://doi.org/10.62754/joe.v3i7.4647

For the period from 2020 to 2080, the changes in land cover groups are shown in Table 8 and Figure 7. The study indicates that urban development is expected to increase from 2,481.95 km² to 12,508.17 km². This growth reflects a significant expansion in urban areas, highlighting the ongoing trends in urbanization and their potential impacts on land use and the environment.

The changes in land cover categories from 2020 to the year 2100 are illustrated in Table 9 and Figure 7. The analysis projects that the built-up area will rise by 13,865.82 km² compared to 2020. This significant increase highlights the ongoing urban expansion and its potential implications for land use and environmental dynamics in the region.

## Conclusions

The low-folded zone is one of the major parts of the Republic of Iraq. It represents parts of eight important Iraqi governorates. These governorates are Diyala, Erbil Kirkuk, Maysan, Ninawa, and Wasit, In addition, it is acknowledged as an important biodiversity hotspot in Iraq.

To have a better grasp on these historical, contemporary, and future spatial changes, this study utilized an integrated strategy that included remote sensing, GIS, and the earth's surface the modeler MOLUSCE. The study's overarching goal was to employ these technologies to foretell how the low folded zone's LULC classifications will change in 2040,2060, 2080, and 2100.

To continuously monitor and assess the changes in LULC over geography and time, remote sensing and geographic information systems offer a valuable opportunity. By employing these methods, the research can provide light on the anticipated LULC changes in the low folded zone. The study draws attention to notable changes in LULC, especially in urbanization and the growth of built-up regions after the year 2000.

In the years 2040, 2060, 2080, and 2100, the study projects that the low folded zone will undergo significant urbanization. Because they shed light on the biological effects and possible degradation of the low folded zone landscape, these results are important for stakeholders, biodiversity conservationists, and decision-makers. However, other landscape fabrics, such as arable land and desert land, would suffer as a result of these developments. The results of the validation K (overall)= 0.83499, K(location)= 0.8586, K(histo) = 0.97245, % of correctness =93.044, and $R^2$= 0.9997 demonstrated a high level of concordance between the classed maps and the maps generated by the model. Future predictions demonstrate that built-up land will increase (from 2481.95 to 16347.77 km²), barren land, water bodies, Dense vegetation, Sparse vegetation, Plantation, and Agricultural fallow and Agricultural land will decrease (from 22595.4 to 19129.18 km²), (from 672.1 to 562.29 km²), (from 1059.83 to 425.73 km²), (from 962.50 to 320.20 km²), (from 1196.75 to 428.5 km²), (from 15172.0389 to 10644.1551 km²) and (from15877.071 to 12408.32 km²) respectively.

The study provides reliable historical data for sustainable land exploitation that minimizes impacts on biodiversity and landscapes. The forecasted LULC maps in 2040, 2060, 2080, and 2100 are useful for this purpose. All planning, decision-making, sustainable management, and preservation of biodiversity endeavors will be guided by these maps. They help lawmakers strike a balance between development and environmental preservation by shedding light on future land use.

## References

Karki S, Thandar AM, Uddin K, Tun S, Aye WM, Aryal K, Kandel P, Chettri N (2018) Impact of land use land cover change on ecosystem services: a comparative analysis on observed data and people's perception in Inle Lake, Myanmar. Environ Syst Res 7:25

Lambin EF, Meyfroidt P (2011) Global land use change, economic globalization, and the looming land scarcity. Proc Natl Acad Sci 108:3465–3472

He C, Liu Z, Gou S, Zhang Q, Zhang J, Xu L (2019) Detecting global urban expansion over the last three decades using a fully convolutional network. Environ Res Lett 14:034008

Journal of Ecohumanism
2024
Volume: 3, No: 7, pp. 2417 – 2433
ISSN: 2752-6798 (Print) | ISSN 2752-6801 (Online)
https://ecohumanism.co.uk/joe/ecohumanism
DOI: https://doi.org/10.62754/joe.v3i7.4647

Seto KC, Güneralp B, Hutyra LR (2012) Global forecasts of urban expansion to 2030 and direct impacts on biodiversity and carbon pools. Proc Natl Acad Sci 109:16083–16088

Diba, Ghonchepour., Amir, Sadoddin., Abdolrassoul, Salmanmahiny., Abdolreza, Bahremand., Anthony, Jakeman., Barry, Croke. (2023). Detection and prediction of land use changes and population dynamics in the Gorganrud River basin, Iran. Land Degradation & Development, doi: 10.1002/ldr.4662

Rizwan, Muhammad., Wenyin, Zhang., Zaheer, Abbas., Feng-Ying, Guo., Luc, Gwiazdzinski. (2022). Spatiotemporal Change Analysis and Prediction of Future Land Use and Land Cover Changes Using QGIS MOLUSCE Plugin and Remote Sensing Big Data: A Case Study of Linyi, China. Land, doi: 10.3390/land11030419

Muhammad, Asif., Jamil, H., Kazmi., Aqil, Tariq., Na, Zhao., Rufat, Guluzade., Walid, Soufan., Khalid, F., Almutairi., Ayman, El, Sabagh., Muhammad, Hasnain, Aslam. (2023). Modelling of Land Use and Land Cover changes and prediction using CA-Markov and Random Forest. Geocarto International, doi: 10.1080/10106049.2023.2210532

manikandan, kamaraj. (2022). Predicting the future land use and land cover changes for Bhavani basin, Tamil Nadu, India, using QGIS MOLUSCE plugin. Environmental Science and Pollution Research, 29(57):86337-86348. doi: 10.1007/s11356-021-17904-6

Soares-Filho, B.S.; Cerqueira, G.C.; Pennachin, C.L. dinamica—A stochastic cellular automata model designed to simulate the landscape dynamics in an Amazonian colonization frontier. Ecol. Model. 2002, 154, 217–235. [CrossRef]

Chen, Z.; Huang, M.; Zhu, D.; Altan, O. Integrating Remote Sensing and a Markov-FLUS Model to Simulate Future Land Use Changes in Hokkaido, Japan. Remote Sens. 2021, 13, 2621. [CrossRef]

Liu, X.; Sun, R.; Yang, Q.; Su, G.; Qi,W. Simulating urban expansion using an improved SLEUTH model. J. Appl. Remote Sens.2012, 6, 061709. [CrossRef]

Pahlavani, P.; Omran, H.A.; Bigdeli, B. A multiple land use change model based on artificial neural network, Markov chain, and multi objective land allocation. Earth Obs. Geomat. Eng. 2017, 1, 82–99.

Rahman, M.T.U.; Tabassum, F.; Rasheduzzaman, M.; Saba, H.; Sarkar, L.; Ferdous, J.; Uddin, S.Z.; Islam, A.Z.M.Z. Temporal dynamics of land use/land cover change and its prediction using CA-ANN model for southwestern coastal Bangladesh. Environ. Monit. Assess. 2017, 189, 1–18. [CrossRef] [PubMed]

Cheng, L.; Sun, H.; Zhang, Y.; Zhen, S. Spatial structure optimization of mountainous abandoned mine land reuse based onsystem dynamics model and CLUE-S model. Int. J. Coal Sci. Technol. 2019, 6, 113–126. [CrossRef]

Pu, R. Mapping Tree Species Using Advanced Remote Sensing Technologies: A State-of-the-Art Review and Perspective. J. RemoteSens. 2021, 2021, 9812624. [CrossRef]

Li, X.; Chen, Y.; Liu, X.; Xu, X.; Chen, G. Experiences and issues of using cellular automata for assisting urban and regional planning in China. Int. J. Geogr. Inf. Sci. 2017, 31, 1606–1629. [CrossRef]

Ngie, A.; Abutaleb, K.; Ahmed, F.; Taiwo, O.-J. Spatial modelling of urban change using satellite remote sensing: A review. Life Chang. Urban Landsc. 2013, 1, 3. [CrossRef]

49. Gomes, E.; Banos, A.; Abrantes, P.; Rocha, J.; Schläpfer, M. Future land use changes in a peri-urban context: Local stakeholder views. Sci. Total Environ. 2020, 718, 137381. [CrossRef]

Paulos, Lukas., Assefa, M., Melesse., Tadesse, Kenea. (2023). Prediction of Future Land Use/Land Cover Changes Using a Coupled CA-ANN Model in the Upper Omo-Gibe River Basin, Ethiopia. Remote sensing, doi: 10.3390/rs15041148

Tamiminia, H.; Salehi, B.; Mahdianpari, M.; Quackenbush, L.; Adeli, S.; Brisco, B. Google Earth Engine for geo-big data applications: A meta-analysis and systematic review. ISPRS J. Photogramm. Remote Sens. 2020, 164, 152–170. [CrossRef]

Lillesand, T.; Kiefer, R.; Chipman, J. Remote Sensing and Image Interpretation, 6th ed.; John Wiley & Sons: Hoboken, NJ, USA, 2015.

Nagendra, H.; Lucas, R.; Honrado, J.P.; Jongman, R.H.; Tarantino, C.; Adamo, M.; Mairota, P. Remote sensing for conservation

monitoring: Assessing protected areas, habitat extent, habitat condition, species diversity, and threats. Ecol. Indic. 2013, 33, 45–59.[CrossRef].

Halmy, M.W.A.; Gessler, P.E.; Hicke, J.A.; Salem, B. Land use/land cover change detection and prediction in the north-western coastal desert of Egypt using Markov-CA. Appl. Geogr. 2015, 63, 101–112. [CrossRef]

Perovic´, V.; Jakšic´, D.; Jaramaz, D.; Kokovic´, N.; C˘ akmak, D.; Mitrovic´, M.; Pavlovic´, P. Spatio-temporal analysis of land use/land cover change and its effects on soil erosion (Case study in the Oplenac wine-producing area, Serbia). Environ. Monit. Assess. 2018,190, 1–18. [CrossRef] [PubMed]

Satya, B.A.; Shashi, M.; Deva, P. Future land use land cover scenario simulation using open source GIS for the city of Warangal,Telangana, India. Appl. Geomatics 2020, 12, 281–290. [CrossRef]

Hatem, K., Al-Jiburi., Naseer, H., Al-Basrawi. (2012). Hydrogeology of the low folded zone.

Liang S, Fang H, Morisette JT, Chen M, Shuey CJ, Walthall CL, Daughtry CS (2002) Atmospheric correction of Landsat ETM+ land surface imagery. II Validation and applications. IEEE Trans Geosci Remote Sens 40:2736–2746

Hakim, A. M. Y., Baja, S., Rampisela, D. A., & Arif, S. (2019, June). Spatial dynamic prediction of landuse/landcover change (case study: tamalanrea sub-district, makassar city). In IOP Con¬ference Series: Earth and Environmental Science (Vol. 280, No. 1, p. 012023). IOP Publishing.

Rahman, M., Tabassum, F., Rasheduzzaman, M., Saba, H., Sarkar, L., Ferdous, J., & Zahedul Islam, A. Z. M. (2017). Temporal dynamics of land use/land cover change and its prediction using CA-ANN model for southwestern coastal Bangladesh. Environmental Monitoring and Assessment, 189(11), 1–18

Ashaolu, E. D., Olorunfemi, J. F., & Ifabiyi, I. P. (2019). Assessing the spatio-temporal pattern of land use and land cover changes in Osun drainage basin, Nigeria. Journal of Environmental Geography, 12(1–2), 41–50.

Journal of Ecohumanism
2024
Volume: 3, No: 7, pp. 2417 – 2433
ISSN: 2752-6798 (Print) | ISSN 2752-6801 (Online)
https://ecohumanism.co.uk/joe/ecohumanism
DOI: https://doi.org/10.62754/joe.v3i7.4647

Guidigan, M. L. G., Sanou, C. L., Ragatoa, D. S., Fafa, C. O., & Mishra, V. N. (2019). Assessing land use/land cover dynamic and its impact in Benin Republic using land change model and CCI-LC products. Earth Systems and Environment, 3(1), 127–137.

El-Tantawi, A. M., Bao, A., Chang, C., & Liu, Y. (2019). Monitoring and predicting land use/cover changes in the Aksu-Tarim River Basin, Xinjiang-China (1990–2030). Environmental Monitoring and Assessment, 191(8), 1–18.

Saputra, M. H., & Lee, H. S. (2019). Prediction of land use and land cover changes for north Sumatra, Indonesia, using an artificial-neural-network-based cellular automaton. Sustainability, 11(11), 3024

Bhattacharya, R. K., Chatterjee, D., N., & Das, K. (2021). Land use and land cover change and its resultant erosion susceptible level: an appraisal using RUSLE and logistic regression in a tropical plateau basin of West Bengal, India. Environment Development and Sustainability, 23(2), 1411–1446.

Akbar TA, Hassan QK, Ishaq S, Batool M, Butt HJ, Jabbar H (2019) Investigative spatial distribution and modeling of existing and future urban land changes and its impact on urbanization and economy.Remote Sens 11:105.